High Efficiency X-Band 50MW Klystron Study

Brandon Weatherford, Valery Dolgashev and Jeff Neilson
SLAC National Accelerator Laboratory, Menlo Park, CA

Aaron Jensen
Leidos, Inc., Billerica, MA

SLAC-R-1096
October 17, 2018

Prepared for CERN under program SLAC 391 - Appendix 19
by SLAC National Accelerator Laboratory.

Table of Contents:

Introduction

SLAC has performed a design study in collaboration with CERN to determine the maximum efficiency that can be achieved in a 50 MW, short pulse (~1 usec), 12 GHz klystron. The design approach was based on recently developed beam bunching techniques [1-3] for modification of bunch core oscillation lengths through appropriate rf cavity design. This study was limited to the design of the gain cavity parameters to achieve high efficiency beam bunching and an output cavity structure to extract the modulated beam power at high efficiency with sustainable surface fields. The magnetic field profile, generation of injected electron beam and collection of the spent electron beam were not addressed.

Design of High Efficiency Bunching Cavities

The first part of this effort was design of the klystron gain circuits for maximum efficiency. First, a baseline COM (Core Oscillation Method) design was established using SLAC's AJDisk and CERN's KlyC-2D klystron simulation codes. Then, the impact of various klystron parameters on efficiency was investigated. After the COM circuit was completed, the bunched beam arising from this circuit was used to redesign the output cavity for increased RF efficiency while minimizing surface gradients in the multiple-gap circuit.

The design targets for the COM klystron circuit were as follows:

- Operating frequency: 12 GHz
- Minimum peak output power: 40 MW
- Goal peak output power: 50 MW
- DC-RF efficiency: 70 percent
- Variables: Perveance, fill factor, klystron length, cavity tunings & positions

Simulation Tools and Circuit Design Approach

The initial design work was carried out using SLAC's AJDisk, to build familiarity with the COM design technique and quickly converge on a "rough" circuit design. As a starting point, a klystron model was constructed based on a COM version of the existing 40 MW SLAC XL-5 klystron, with an identical beam tunnel diameter, perveance, and fill factor. The design was scaled in beam power (to 71.4 MW, assuming 70% efficiency), with the perveance held constant at 1.23 μK. Cavity positions and tunings were manually adjusted for maximum efficiency. The final simulation from this procedure yielded 57.7 MW of output power for a total efficiency of 81 percent in AJDisk, however this was viewed as an unrealistic "best-case" design. The result is shown in Figure 1.

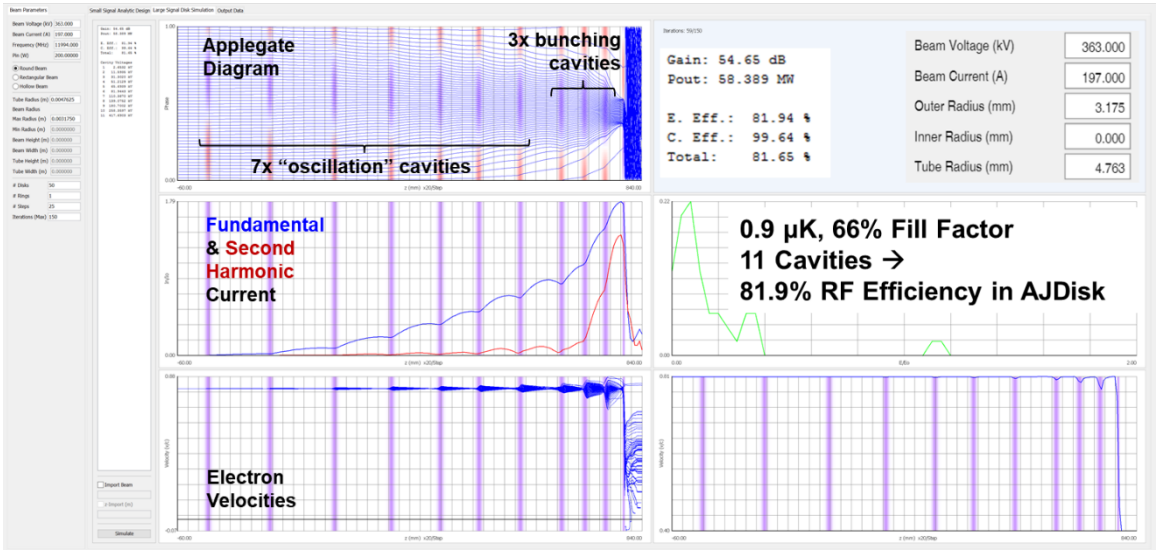

Figure 1. AJDisk simulation results of the preliminary baseline design – 0.9 µK, 66% fill factor, 11-cavities, with an ideal output.

A rough design process was established from these early AJDisk simulations; mostly related to cavity placement and tunings to prevent aggressive bunching of the beam and velocity spread. This was used as a guide to quickly establish an initial model for optimization runs in KlyC. This procedure is documented in a previous informal report to CERN. Once the baseline design from AJDisk was ported over to KlyC, all further work was done in KlyC.

Baseline COM Design with 11 Cavities

Each variation of the klystron circuit in this report was developed in three phases using KlyC. The first phase was to recreate the rough design from AJDisk in KlyC, with an idealized output cavity to isolate the effect of the bunching circuit on the RF efficiency. The output cavity was set with an unrealistically large M-factor of 0.9, while it was expected that in the final design, M=0.7 was a more realistic target. The rough design was run in KlyC-1D to confirm that the solution agreed with AJDisk. This model was then used as an initial setup for a KlyC-2D optimization, using four layers to account for radial stratification effects. A maximum efficiency design was determined using the local optimizer routine in KlyC, with the optimizer limited to small perturbations in cavity positions and tunings. The resulting four-layer design was then re-solved using 10 layers for final confirmation, though the resulting impact on efficiency was usually a fraction of a percent.

The results of the baseline design in KlyC-2D are shown in Figure 2 below. This design has 11 cavities – seven "oscillation" cavities, three "bunching" cavities near the output, and the output cavity itself. The perveance was reduced from the standard XL5 tube (to 0.9 µK), with an operating voltage of 363 kV. The fill factor was kept at 66%, and the beam tunnel radius was 4.76 mm.

Each color in the plots below represents a separate radial layer, with blue at the outer edge of the beam and red at the innermost radius. The harmonic current plots show that for this optimized

high efficiency case, the outer edge of the beam reaches saturated harmonic current level at three cavities before the output, while the innermost radius continues to be bunched until the final cavity. The Applegate diagram confirms this radial variation with the outer layer converging to the central phase much more rapidly than the inner layer; the velocity plots also manifests these 2-D effects with a spread in velocity versus radius. The resulting output power for this starting design was 56 MW, with 54.5 dB of gain, and an electronic efficiency of 78.5%.

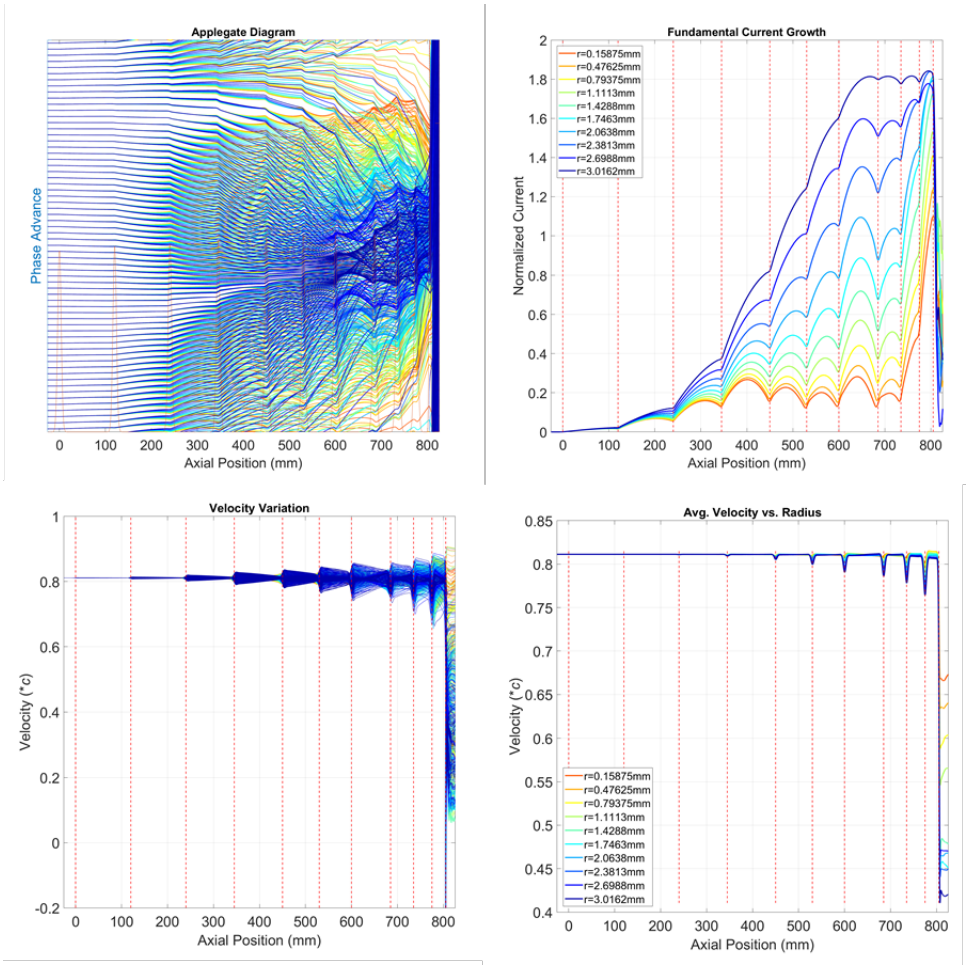

Figure 2. KlyC-2D results for optimized 11 cavity COM circuit.

Variable Perveance and Fill Factor

The same design process, with a 1-D design followed by 2-D optimization and confirmation using 10 layers, was repeated for different fill factors and perveance values; examples are shown in Figure 3. The baseline design is shown in the middle; the design on the left had an increased fill factor of 75%, while the design on the right had an increased perveance of 1.5 μK. All other variables were unchanged.

The optimized design with a slightly higher fill factor was longer than the baseline design, but the final ratio of outer to inner harmonic current densities was improved from 1.67 to 1.32. The

resulting efficiency, however, only increased from 78.5 to 79.4 percent, and this is likely not worth the added design risk of higher fill factor.

The higher perveance design was substantially shorter (600 mm versus 805 mm for the baseline), with the outer layer reaching full saturation at 400 mm. The high perveance design showed some divergence between outer and inner harmonic current growth, with the harmonic current in the inner layer actually decreasing over the second half of the tube. The increased variation in harmonic current density versus radius at the output cavity leads to a reduced efficiency of 72.6% for this design.

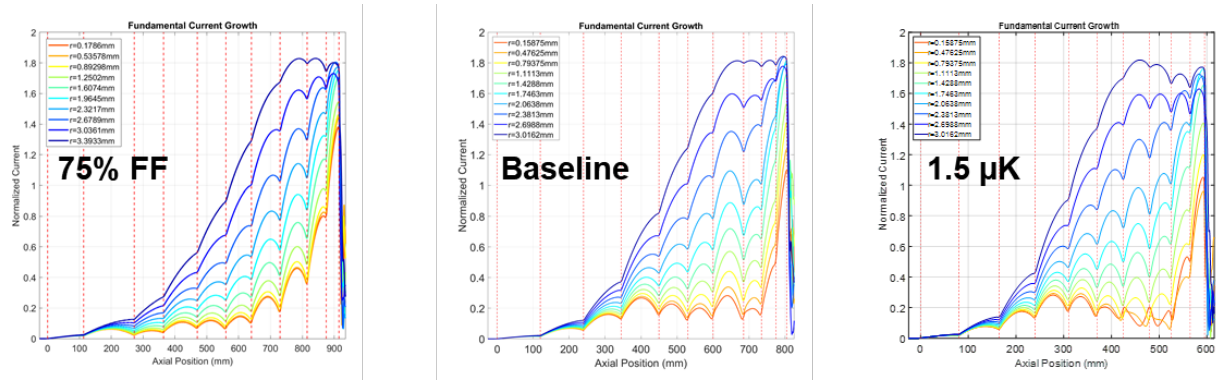

Figure 3. Harmonic current profiles from KlyC-2D, for variable perveance and fill factor, with ideal output. Left: 0.9 µK, 75% FF, 79.4% Efficiency. Middle: Original baseline – 0.9 µK, 66% FF, 78.5% Efficiency. Right: 1.5 µK, 66% FF, 72.6% Efficiency.

9-Cavity Optimized Design

In all three design variations, the harmonic current and Applegate diagrams clearly show that the number of cavities can be reduced without much sacrifice to harmonic current, which is mostly carried at the outer edge of the beam. As a result, a new design with 0.9 µK and 66% fill factor was developed with only 9 cavities. The optimization process was repeated for this circuit, and the result is shown in Figure 4.

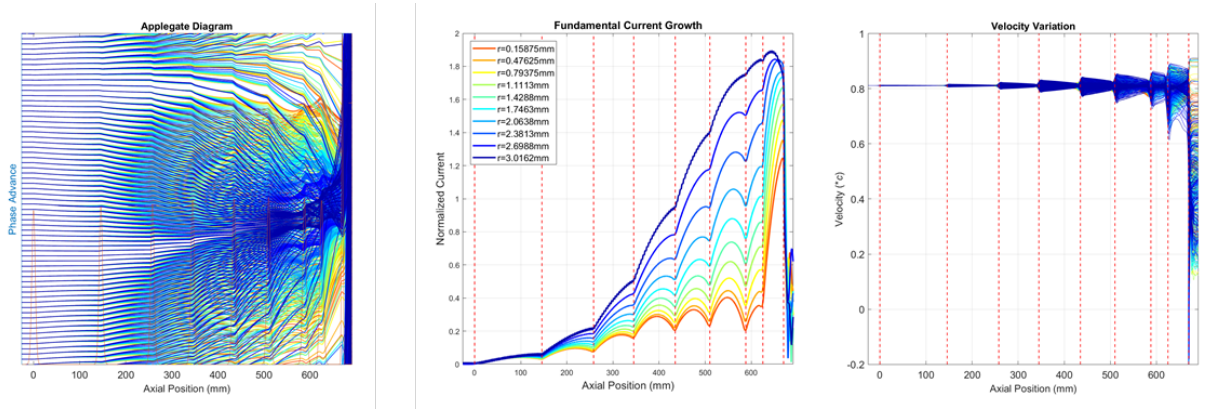

Figure 4. Finalized bunching circuit design: 9 cavities, 0.9 µK, 66% FF. 76% Efficiency with ideal output

For the 9-cavity design, the harmonic current now peaks directly at the output, but the radial current variation is comparable to the 11-cavity design. The Applegate diagram shows all phases converging at the final cavity, rather than in the 11-cavity design where the outer layer went through three oscillations over the last three cavities. The efficiency was slightly reduced by this design change, from 78.5% to 76.0%, but the length of the device was reduced substantially from 805 mm to 670 mm. As this was a relatively small reduction in efficiency, the 9-cavity design was taken as the new baseline moving forward.

Finally, the optimized 9-cavity bunching circuit was simulated using 10 layers, but with a more realistic output cavity gap coupling factor (M = 0.75) and the cavity tuned for maximum efficiency. First, the optimized 9-cavity circuit was imported into AJDisk, and the tube was simulated over a range of M-factors and output cavity frequencies. The optimal output cavity was chosen (with a predicted efficiency of 74.5% in AJDisk), and the cavity parameters were then used in the 10-layer KlyC-2D simulation. The result (Figure 5), with an electronic efficiency of 70.7%, suggested that efficiencies around 70% should be achievable with this optimized COM circuit. Therefore, this 9-cavity bunching circuit would be simulated in MAGIC-2D, to generate a COM-like electron bunch that could be imported directly for final optimization of the multi-gap output circuit.

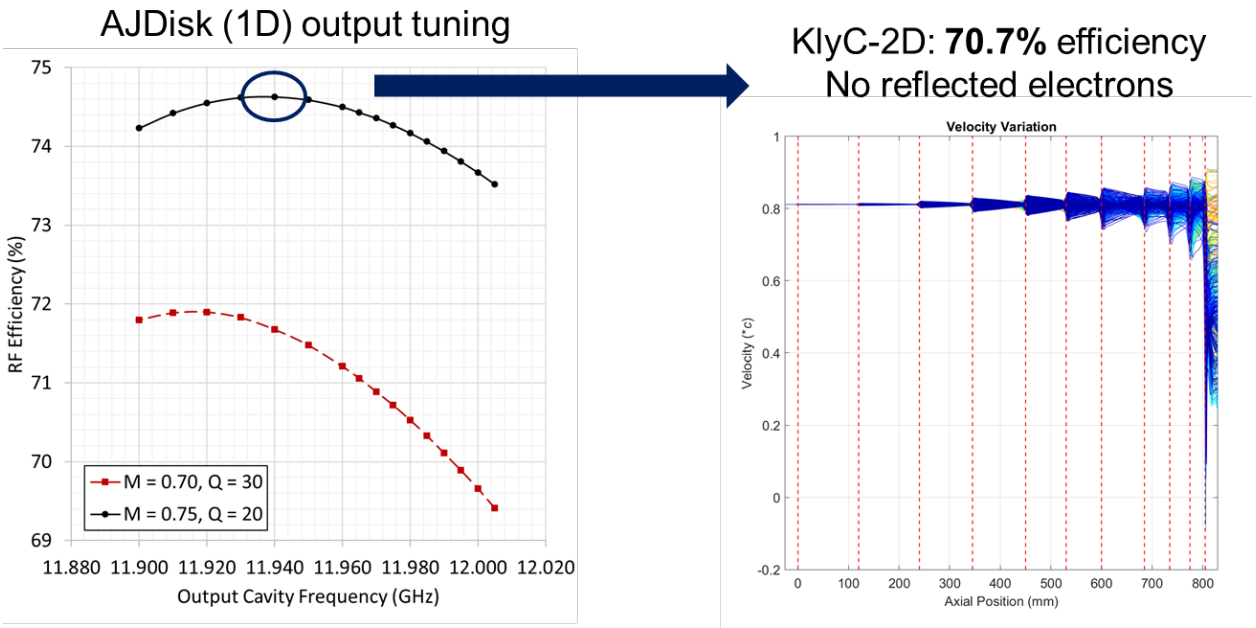

Figure 5. Left: Efficiency vs. output cavity parameters for 9-cavity design, in AJDisk. Right: resulting velocity distribution when using realistic output cavity with M=0.75.

During the review of the COM design, it was discovered that the klystron had a gain of 97dB at a few hundred megahertz above the operating frequency (Figure 6). Initially, this was corrected by spoiling the cavity R/Qs and adjusting the cavity frequencies. Finally, it was determined that instabilities due to high gain would be related to reflected particles from the output cavity which would only occur if the tube were operated at a frequency where the high gain occurred. Since the tube is operated at a lower frequency and gain we expect the tube to be stable even if a high gain exists at a higher frequency than the operating frequency.

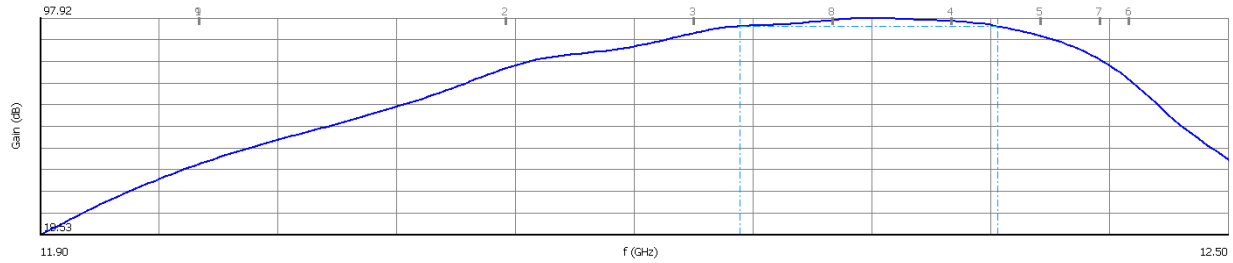

Figure 6 Gain versus frequency for the initial COM design

Output Circuit Design

Mode Selection

The 0, π, and $\pi/2$ modes were considered for the output structure. The three modes were simulated in Superfish as shown in Figure 7. The 0 mode has very low coupling with a spacing of only 309kHz between the 0 and π mode, making it unusable for the X-band COM klystron. The standing wave π mode is more attractive with a coupling coefficient ~0.7 and 30.7MHz between the 0 and π mode. In the π mode the real output structure will require at least four cells resulting in a mode to mode spacing < 10MHz. For this reason, the design study will focus on use of the $\pi/2$ traveling wave mode with several cells to reduce the peak surface gradients. Having more cells will make achieving stability more challenging which could give the π mode enough merit to study further at some point in the future.

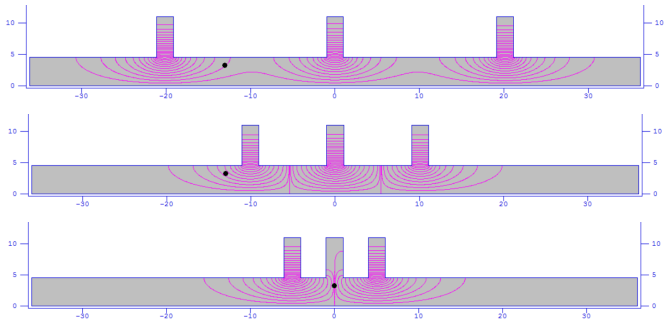

Figure 7 Electric field configuration for three modes. (a) 0 mode ($f_\pi - f_{2\pi} = 309$kHz) (b) π mode ($f_\pi - f_{2\pi} = 30.7$ MHz) (c) π /2 mode ($f_\pi - f_{2\pi} = 335.8$MHz)

1D Optimization of the Output Structure

Modeling of complex fields in AJDISK was added to allow rapidly analysis and optimization of the output structure in 1D. This approach will not properly model the effects of radial stratification but does provide a baseline design from which a 2D model can be developed. The complex field is generated synthetically using a python script. The complex field is modeled as a series of half sine waves whose amplitude and phase advance are controlled by the optimization. The phase advance is set to approximately $\pi/2$ but allowed to vary such that it best matches the decelerating beam velocity.

The optimization was done using Sandia National Laboratory's "Dakota" library. The Dakota optimization is managed by the Galaxy Simulation Builder (GSB) software developed by the Air Forces Research Laboratory (AFRL). The optimizations are all done using the genetic algorithm

which is a global optimization routine. To facilitate this process a python script was created to define the field profile and phase over the length of the structure as second order functions. In this way the output structure can be modeled with any number of cells without increasing the number of variables to be optimized over. It also ensures smooth variation in field amplitude and phase advance over the length of the structure.

The results of optimizing output structures with one up to five cells are shown in Figure 8. As would be expected, the peak gradient decreases as more cells are added. An initial on-axis field gradient bound of <40MV/m was set to achieve sustainable surface gradients assuming a maximum field gradient target of <100 MV/m. This ratio assumption was based on those typically obtained for optimized accelerator cells. This initial optimization achieved 88% efficiency but still exceeded 40MV/m. Based on these results it is clear the structure will need more than five cells. However, as the analysis progressed it was also realized that the upper bound on-axis field gradient was chosen too high and should be <20 MV/m, which is discussed in latter section of this report.

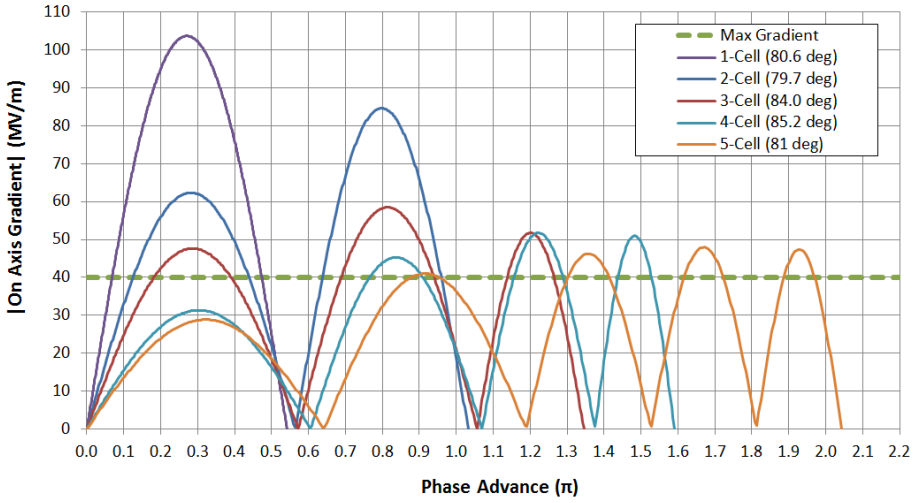

Figure 8 On axis gradients for one to five-cell optimization

To further increase the fidelity of the field profile model, a pure traveling wave term of amplitude α was added:

$$E_n(x) = A_n \frac{\sin\left(\frac{\pi x}{d}+\frac{\pi}{2}\right)e^{i\frac{\pi}{2}n} + \alpha\, e^{-i\left(\frac{\pi x}{2d}+\frac{\pi}{2}n\right)}}{1+\alpha} \quad (1)$$

where n is the cell number, x is the relative location within the cell, and d is the total cell length. This term is a second order effect that better models the field profile of a real traveling wave structure.

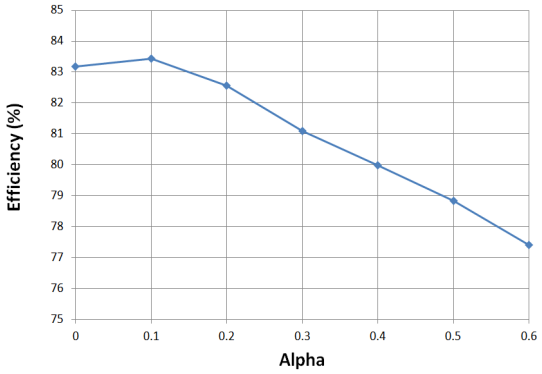

Figure 9 Six-cell output efficiency versus alpha

Using Eqn. 1 to optimize a six-cell structure with α equal to zero the efficiency dropped to 83%. The same six cell structure was simulated versus α for this optimized case as shown in Figure 9. The efficiency is somewhat insensitive to α. It is believed that the efficiency drops with increasing α simply because the design was optimized for an α of zero.

At this point in the study a representative single cell (d = 3mm) geometry was designed and simulated in HFSS (Figure 10). The surface field calculation showed the surface to on-axis field ratio for this cell geometry is approximately five so the on-axis field gradient limit used in the previous optimizations was too low. The last cell in the output structures is fairly short so there is likely little room for improving the surface to peak ratio, but shaping of the cell noses could be investigated to see if any reduction is possible during a 2D design effort. For further cell optimizations a new goal of 20MV/m has been set for the maximum axial field. Since the 1D axial field is the average of the axial field across the beam radius the maximum surface field will be less than five times higher.

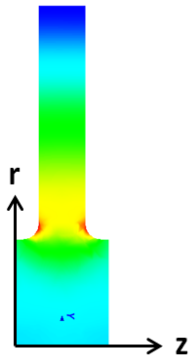

Figure 10 Complex field amplitude for d = 3mm.

The optimization was modified to include the new field model and a slowly increasing penalty for fields over 18MV/m on axis. Initial optimizations varied both cell length and cell amplitude with a fixed α and final optimization used constant cell amplitudes. The maximum on-axis field gradient was significantly reduced (<20 MV/m) from the initial standing wave calculation without a significant impact on efficiency for designs with six cells or more. For fewer cells the reduced gradients significantly impacted efficiency. Figure 11 shows efficiency versus the number of output cells with the gradient penalty included.

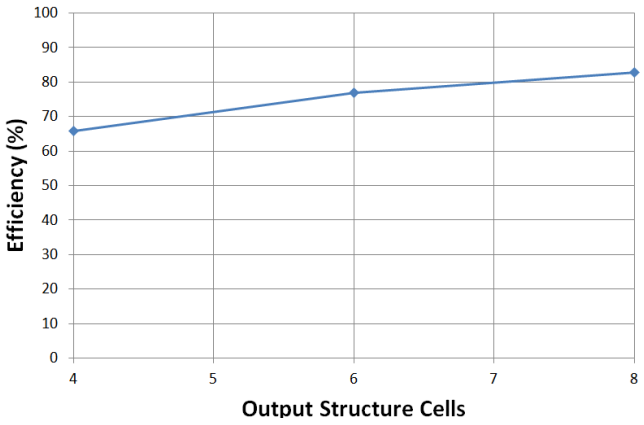

Figure 11 Efficiency vs. number of cells. Optimized with a penalty for structures exceeding 18MV/m.

2D/3D Design and Optimization Using Synthetic Beam

3D design and optimization were performed using Neptune, a 3D FDTD PIC code with GPU acceleration from the US Naval Research Laboratory (NRL). A typical 3D simulation of the seven-cell output structure being designed took approximately10 minutes wall clock time. Unfortunately, NRL has asked that results and images from Neptune not be shared since Neptune has not been officially released. Since we cannot release the results from the Neptune calculations, the final results from Neptune were ported and simulated in MAGIC2D. We found that the Neptune 3D calculations and MAGIC2D were in good agreement. It is also of note that the Neptune 3D simulation execution time was several times faster than the 2D MAGIC execution times for the same output structure.

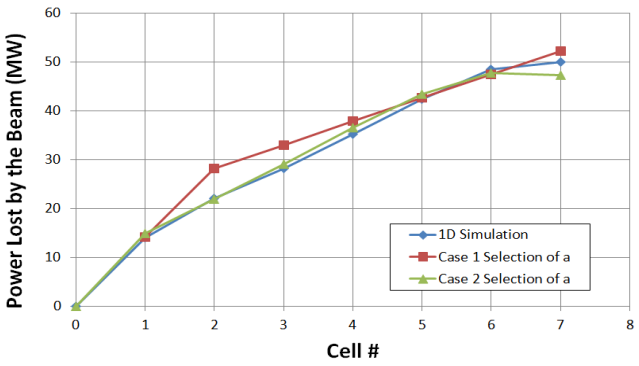

Figure 12 Using the power extracted from the beam to determine the iris dimension a.

The first step in optimizing the geometry in Neptune was translating the 1D results into an initial 2D geometry. The power extracted from the beam versus distance was taken from the 1D simulation. Then iris dimension, *a*, of each cell was adjusted such that, based on impedance, each 2D cell would extract the power observed in the optimized 1D simulation. Figure 12 shows the power extracted from the beam in the 1D simulation versus two different sets of iris values.

Each cell's frequency was tuned using cell radius such that it would operate in the $\pi/2$ mode. The simulation of cell frequency was done using two half cells as shown in Figure 13a with a master slave boundary. This assumes a constant iris dimension as shown in Figure 13b. The best fit curve for the $\pi/2$ mode is given by

$$r = (-0.075202 * a + 0.091672) * d + (1.050311 * a + 7.248257) \quad (2)$$

where *a* is the iris dimension in millimeters, *d* is the cell period in millimeters, and *r* is the cell radius in mm. The iris thickness, *t*, was assumed to be 1.4mm.

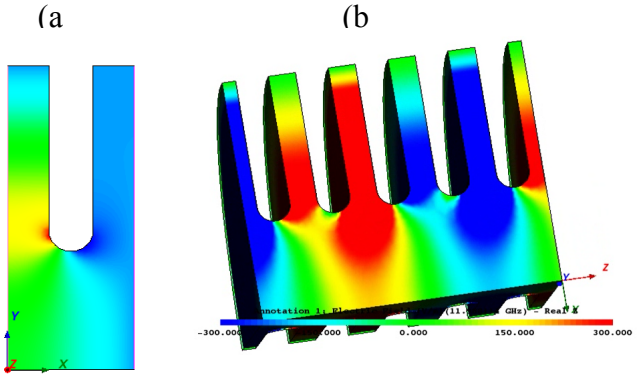

Figure 13 RF simulations used to calculate the π/2 cell frequency. (a) 2D half-cell geometry using master slave boundaries. (b) The same model in 3D with multiple cells

The geometry of the output cell used for optimization in Neptune was adapted from the design of the XL-5 klystron. The seven cell 3D geometry is shown in Figure 14 including the output cell geometry and coupler. The output cell height and iris opening to the output waveguide (effectively the frequency and external Q) were both included as variables in the 3D optimization runs.

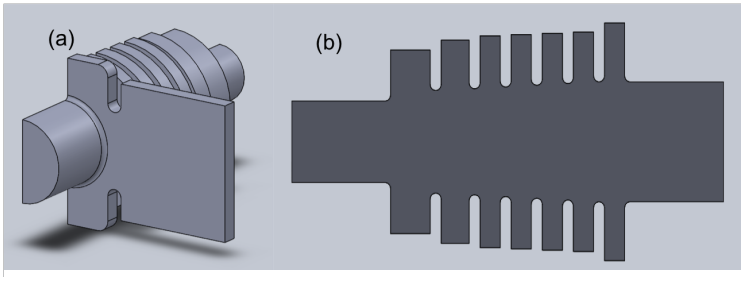

Figure 14 Geometry of the sevel cell output structure used for optimization. (a) Output power extraction cell with coupling waveguide. (b) Crossection of complete seven cell geometry

Due to the sensitivity of the design to cell frequency and the slow execution of 3D simulations the optimization using Neptune used a local optimization. Figure 15 shows an example optimization run as viewed in GSB. The first iterations are shown using blue lines and change to red lines as the optimization converges. Each line, representing an optimization iteration, shows the normalized value of each variable being optimized and the resulting merit value of the iteration. In the optimization in Figure 15: *a2* is iris radius between the first and second cell, *dyIris* and *dyOutput* are for the output cell, *R1* is the first cell radius, *R2* is the second cell radius, and *RBulk* is a global scaling factor for the cell radius of cells three through six.

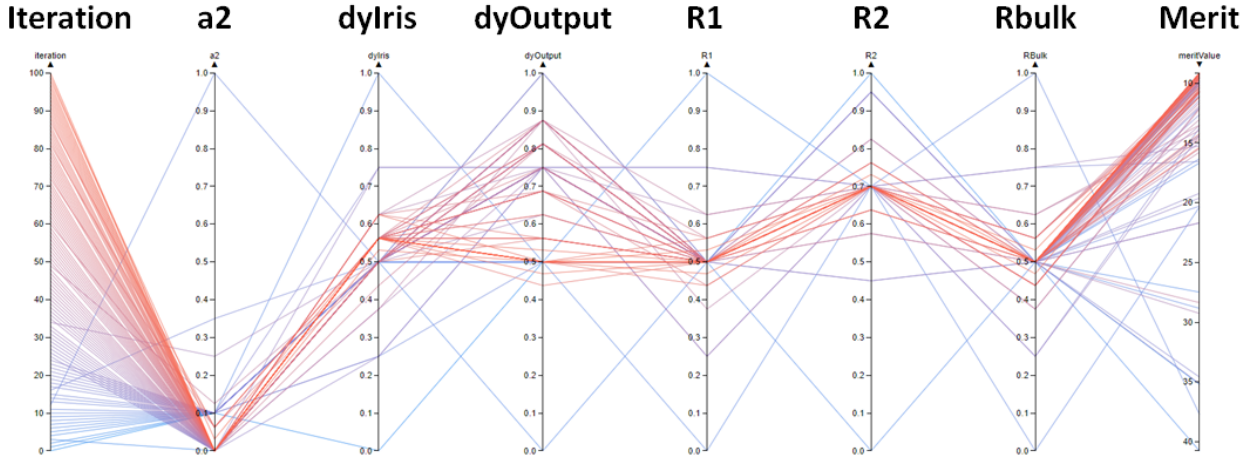

Figure 15 Galaxy Simulation Builder Neptune optimization.

The Neptune optimization runs used a modulated current as described in Equation 3 which is normalized so the integration of *I(t)* over *t* yields *Io*. With this modulated current an output power of 50MW (70% efficiency) was achieved. For the current described in Equation 3 the beam is injected 12mm before the first cell.

$$I(t) = I_0 \frac{\pi}{0.5535393641535147} \sin(\pi f t)^{20} \qquad (3)$$

The frequency of each cell in Neptune was simulated with all adjacent cells shorted out. The cell frequencies are plotted in Figure 16a. The values from input to output of each cell frequency in GHz were: 11.978, 11.376, 11.475, 11.435, 11.400, 11.359, and 11.248. The external Q of the

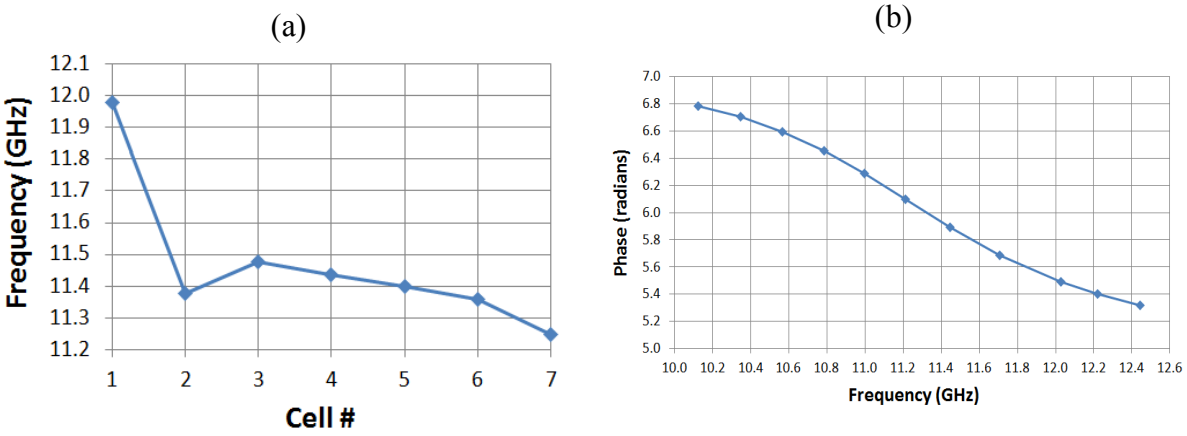

Figure 16 Calculation for cell parameters (a) Frequencies of individual cells. (b) Kroll-Yu phase versus frequency for a moving short in the output waveguide.

last cell was 4.6 based on the Kroll-Yu method using the phase and frequency shown in Figure 16b. The cell periods in millimeters in order from the input to output are: 6.5, 5, 4, 4, 4, 4, and 4.

The optimized geometry obtained using Neptune calculations was simulated exactly without tuning in a MAGIC2D calculation with the exception of the output cell. Since the output cell with coupler is a 3D geometry a "translation" of this cell to 2D was performed by modification of radius used in MAGIC2D model. The 2D cell radius of the last cell in MAGIC2D calculation was set to 12.894mm. This cell radius could not be easily tuned due to the structured grid in MAGIC so the last cell period was also modified by 10% (4mm * 0.9) to get exact frequency match. The beam voltage was 363kV, the beam current was 197A, the beam radius was 3.175mm, and the magnetic field was set to a constant 4kG field over the length of the structure. The MAGIC2D simulation achieved 50MW for the ideal beam bunching described in Equation 3. The RF current and power extracted from the beam in MAGIC2D are plotted in Figure 17.

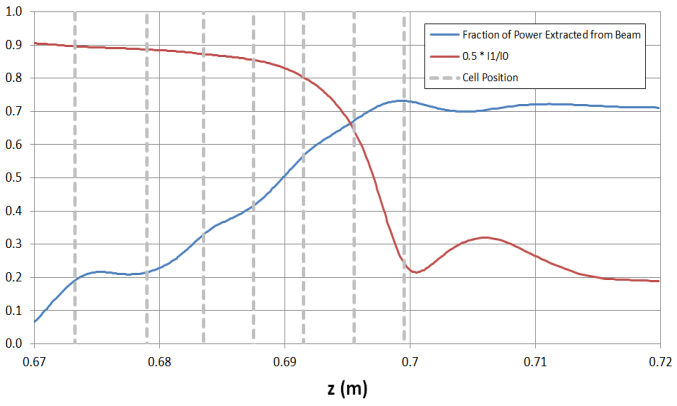

Figure 17 RF current and power extracted from the beam versus distance for a MAGIC2D simulation with 50MW of output power.

2D/3D Design and Optimization Using Realistic Beam Import

The design of the beam bunching cavities and output cavity were done in parallel so initial optimization of the output cavities in 2D/3D were done using an analytic expression for beam current (Eqn. 3). After the bunching cavities designs were completed a series of translators were developed to import the modulated beam data from the codes used to design bunching cavities (AJDISK and KlyC 1 and 2D) to the codes used for output cavity analysis (MAGIC2D and Neptune). Figure 18a shows a typical arrival time plot from KlyC for 1 ring case. Figure 18b shows a KlyC RF current for the beam being imported from KlyC into MAGIC2D and Neptune. This four ring beam case was from a CERN optimized buncher cavity design (*SLACKlystronforCLIC_opt_3.klc*).

(a) (b)

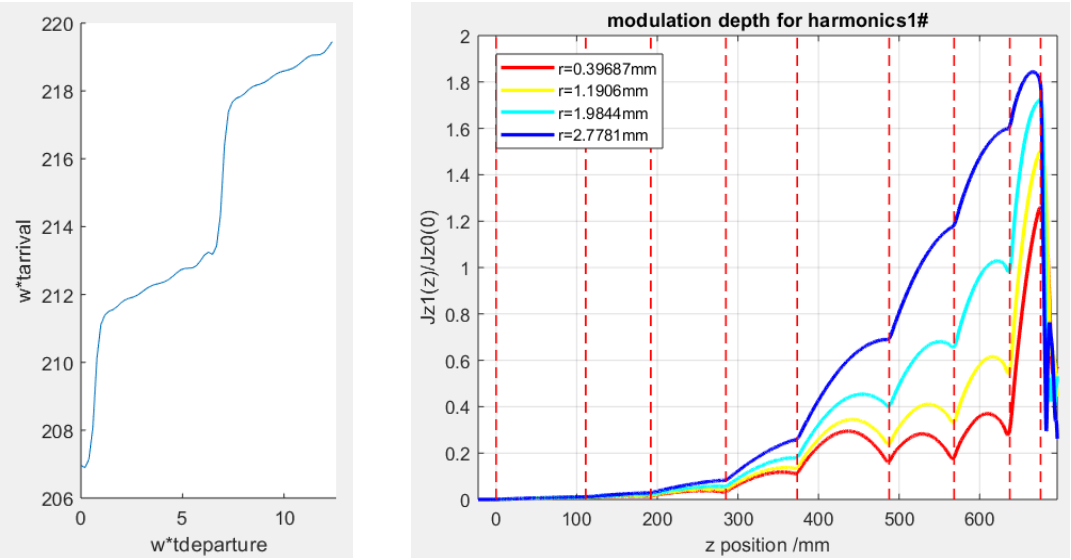

Figure 18 Data used from KlyC calculations is used to build the Neptune and MAGIC2D input beam files. (a) Typical arrival time plot from KlyC for 1 ring. (b) RF current for 4 rings of the beam.

The efficiency calculated using the KlyC imported beams was less than those obtained using analytic beam, producing on the order of 40MW in both MAGIC2D and Neptune codes. The results are shown in Figure 19. It should be noted that the 2D beam performs better than the 1D beam so the reduction in power from the analytical beam bunch is not strictly a 2D effect. It should also be noted that the AJDISK beam uses a different circuit design (the design provided by SLAC) than the KlyC beams (provided by CERN).

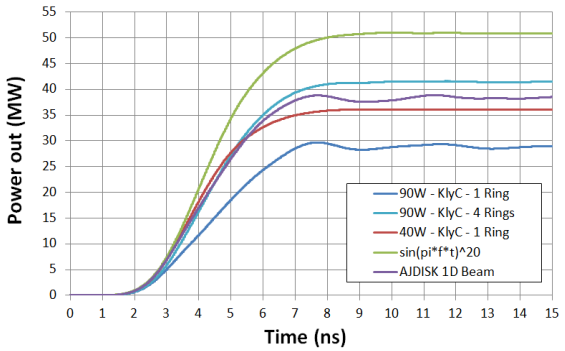

Figure 19 MAGIC2D output power using beams from KlyC and AJDISK

Based on the results shown in Figure 19 the beam bunch and circuit are not optimal for one another. This is not surprising since the design was based on Equation 3. The question is whether or not the beam bunch needs to be reengineered or if simply re-optimizing the circuit for the 2D beam is sufficient. The first two cells in the design are longer in an attempt to match the phase advance to the beam velocity. It is believed that it may be possible to control the phase advance based on cell tuning. For a simple single cell, the phase is tunable using cell radius as shown in Figure 20. The cell radius in the plot is given relative to the cell radius required to tune an isolated single cell with a long beam pipe to 11.994 GHz (analogous to cell tuning when adjacent cells are shorted). Further analysis of the phase is needed to understand the impact of cell radius when incorporated in a coupled multi-cell structure.

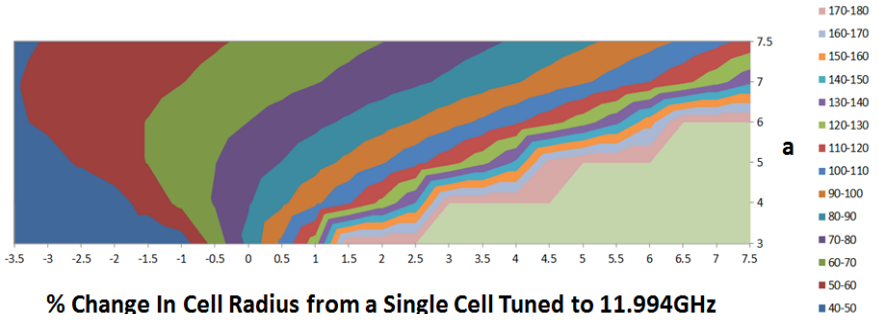

Figure 20 Phase advance of a cell period of 4mm versus cell radius for various iris radii.

The geometry was re-optimized for the 2D KlyC bunch by optimizing the external Q of the final cell and the seven cell radii. The optimization allowed the cell radii and output iris to vary by +/- 3%. The optimized geometry had the following cell frequencies in GHz as shown in Figure 22: 11.926, 11.021, 11.361, 11.436, 11.345, and 11.359. The cell radii in mm were: 10.766mm, 12.181mm, 12.460mm, 12.518mm, 12.716mm, and 12.818mm. The output cell height and iris opening were 27.772mm and 14.951mm respectively. The iris opening was measured from the center of the radiused iris nose. The new structure's output cell frequency and external Q still need to be calculated using the Kroll-Yu method.

The Neptune simulation achieved 47.16MW output power and 65.9% efficiency. The external Q in the optimization was limited by the range the output iris was allowed to change. The optimization was run to near convergence but had to be stopped early due to technical issues. For these reasons it is expected that the output power and efficiency could be increased.

Concluding Remarks

The feasibility of a high efficiency traveling wave structure for a 363kV, 197A, 11.994GHz COM based klystron has been demonstrated. Greater than 70% efficiency and 50MW was demonstrated using a seven-cell geometry in MAGIC2D and the beam bunching described in Equation 3. The peak surface fields for this design were less than 100MV/m. The output structure was re-optimized for the 2D KlyC beam using Neptune/GSB and an output power of 47 MW and 66% efficiency was achieved with a peak surface gradient also less than 100MV/m. The re-optimization optimized the external Q of the final cell and the seven cell radii. The external Q hit an artificial limit during the optimization and the optimization was not run to full

convergence. For these reasons it is expected that the output and efficiency could be optimized to even higher values.

Several tasks could be considered next. It is believed that further optimization of the geometry is possible. A full impedance matrix analysis should be conducted. A study of controlling the phase advance with cell radius in a multi-cell structure would be of interest. It may be possible to replace the first two cells in the seven-cell structure with three 4mm cells to achieve an 8-cell structure consisting of only 4mm cell periods. A six-cell structure consisting of cells with a 5mm period may also be tractable and have lower gradients. We believe it is possible to predict the peak surface gradient a priori by evaluating the peak surface field for the structure in Figure 13a with a fixed power flow of 50MW. A study of peak gradient vs. cell period would be of interest, especially if the phase advance can be controlled by adjusting the cell radius. Reducing gradients in the output structure may be possible by extracting power from not only the output cell but also intermediate cells. Adapting KlyC to optimize the output structure geometry self-consistently would be an ideal optimization tool for further design work.

Pulsed Depressed Collector Technology

Recently SLAC has developed self-biased depressed collector technology [4] for recovering the energy both in the spent beam of the klystron during the rf on part of the pulse along with the lost energy in the rise/fall times of the modulator pulse. This collector technology is very applicable to this klystron development though not so much from the increase in rf efficiency. Because of the potential high interaction efficiency of this klystron, approaching or potentially exceeding 70%, the increase in overall efficiency with introduction of a depressed collector will be modest (see Figure 21). A larger savings would be achieved in capturing the energy in the rise/fall times of the modulator pulse. The amount of energy lost in the rise/fall time of a pulse with 1 usec flat-top from a typical modulator is on the order of 30%. Assuming a conservative 60% recovery of this energy, there will be approximately double the energy savings in the rise/fall time energy recovery versus that during the rf on part of the pulse (flat portion of pulse).

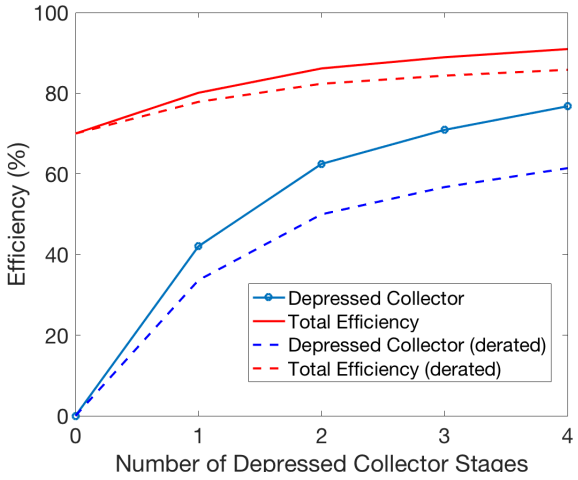

Figure 21 Depressed collector and total rf efficiency versus number of stages in collector for HEX klystron. Theoretical limits are solid line, dashed lines are for empirical based expectation.

The single beam proposed configuration of CLIC as klystron driven accelerator would require 5000, 50 MW klystrons. Assuming 0.01% duty cycle, 5000 operational hours/year and an energy cost of 60 Euro/MW hour the savings from implementing self-biased depressed collector technology on the klystrons would be on the order of 4.5M Euro/year. Additional savings would occur from reduction in cooling costs and capital savings from reduced power plant power requirements and lower costs on modulators since rise/fall time requirements could be relaxed.

References

[1] Syratchev, I., “High Efficiency Klystron Technology,” *International Workshop on Breakdown Science and High Gradient Technology*, Valencia, Spain, 2017

[2] Baikov, A. Y., Marrelli, C., and Syratchev, I., “Toward High-Power Klystrons With RF Power Conversion Efficiency on the Order of 90%,” *IEEE Trans. Electron Devices*, vol. 62, no. 10, p. 3406, 2015.

[3] Guzilov, I. A, “BAC Method of Increasing the Efficiency in Klystrons*,” IEEE Vacuum Electron Sources Conference (IVESC)*, June 20-July 4, 2014

[4] Kemp, Mark A., Aaron Jensen, and Jeff Neilson. "A self-biasing pulsed depressed collector." IEEE Transactions on Electron Devices 61.6 (2014): 1824-1829.